HEFAT2008
6th International Conference on Heat Transfer, Fluid Mechanics and Thermodynamics
30 June to 2 July 2008
Pretoria, South Africa
Paper Number: BE1

Viscous incompressible natural convection/isothermal flows in primitive variables

Elsa Báez and Alfredo Nicolás[1]
[1]*Author for correspondence*
Depto. Matemáticas, 3er. Piso Ed. Diego Bricio
UAM-Iztapalapa, 09340
México D.F. México
E-mail: anc@xanum.uam.mx

ABSTRACT

Natural convection/isothermal flows, described by the unsteady Boussinesq approximation and the Navier-Stokes equations, are studied numerically using a simple projection method, based on an operator splitting, after a convenient time discretization is made. The whole process involves four steps: one for the energy equation (temperature step) and three for the momentum and continuity equations (motion steps). The numerical scheme is independent of the dimension of the space and of the shape of the region where the flow is developed. 2D numerical experiments are reported in rectangular cavities: natural convection flows in cavities filled with air for Raleigh numbers $Ra \leq 10^6$ and isothermal flows in the well known lid-driven cavity problem for Reynolds numbers $Re \leq 1000$.

INTRODUCTION

Natural convection flows modeled by the unsteady Boussinesq approximation and isothermal flows modeled by the unsteady Navier-Stokes equations are studied in this work. The numerical scheme is based on a simple projection method involving an operator splitting of four steps for the temperature, momentum, and continuity equations in the time discretization: From one of the steps the temperature is computed, called the temperature step, and from the second to the fourth step the pressure and the velocity are computed; two of these latter sub-steps involve the computing of two intermediate velocities, one of which satisfies the incompressibility condition, and the solution of a Poisson equation for the pressure with Neumann boundary condition, and the fourth step gives the final velocity through the solution of a vectorial elliptic equation, with Dirichlet boundary condition. Then, the difficulties associated with the non-linearity and the incompressibility constraint are decoupled; no iteration at each time step is required. For isothermal flows the temperature step is eliminated. Although 3D fluid flows can be handled by the numerical method, only 2D flows in rectangular cavities are reported here.

The numerical procedure, in its isothermal restriction, is very close to the one reported in Badalassi et al. [1] for multiphase flows, which are more complicated than the ones considered here, which in turn is close to the one in Karnadiakis et al. [2]; no one of these works considers thermal flows and other discretizations tools, very different of the ones considered here, are used because of their particular needs: high order discretizations in time in [2], spectral methods for the spatial discretization, to handle accurately those more complicated flows, in [1]. A crucial problem to solve efficiently for the pressure is discussed in [2], based on some considerations pointed out before, Orszag [3]; this discussion has been continued, say in [1], Gresho and Sani [4], and Sani et al. [5]. From those discussions, an efficient solution for the pressure seems to be the one obtained by solving a Poisson equation for the pressure, through an operator splitting procedure applied to the whole problem, with an appropriate Neumann boundary condition obtained from the normal projection of the gradient of the pressure in the semi-discrete momentum equation.

The evolution of the natural convection flows presented here depends on the parameter given by the Rayleigh number Ra and that of isothermal type depends on the Reynolds number Re, and both evolutions depend on the aspect ratio A (A=ratio of the height to the width) of the cavity. All the natural convection flows are complemented with the local Nusselt number Nu and the global Nusselt number $\overline{Nu}$ to measure the heat transfer of the flow. With the values of $\overline{Nu}$ and the graph of Nu and some characteristic values of the stream function and/or the components of the velocity the influence of the parameters Ra and A on the evolution of thermal flows, concerning the activity of the fluid motion and of the heat transfer, can be described as well as that of isothermal flows without considering $\overline{Nu}$ and Nu. All the flows we are reporting are asymptotic converged ones to their steady state, then the time T_{ss} when the steady state is reached, according to the discrete absolute stopping criterion in all the cavity, is reported. Then, how T_{ss} varies as Ra, Re, or A varies gives another mean to find out about the activity of the flow. On the other hand, the numerical results are obtained with significant coarse meshes which, together with the fact that no iteration is required, makes the numerical procedure very efficient computationally speaking.

MATHEMATICAL MODEL

Let $\Omega \subset R^N (N = 2, 3)$ be the region of the flow of an unsteady, thermal, viscous, incompressible fluid, and Γ its boundary, this kind of flows can be modeled, in Ω and for $t > 0$, by the dimensionless system

$$\begin{aligned} \mathbf{u}_t + (\mathbf{u}\cdot\nabla)\mathbf{u} + \nabla p &= \tfrac{1}{Re}\nabla^2\mathbf{u} + \mathbf{f} \quad (a)\\ \nabla\cdot\mathbf{u} &= 0 \quad (b) \qquad (1)\\ \theta_t + (\mathbf{u}\cdot\nabla)\theta &= \tfrac{1}{RePr}\nabla^2\theta \quad (c) \end{aligned}$$

known as the Boussinesq approximation if $\mathbf{f} = \frac{Ra}{PrRe^2}\,\theta\,\mathbf{e}$, with $\mathbf{e}$ the unitary vector in the gravitational direction; where $\mathbf{u}$, p, and θ are the velocity, pressure, and temperature of the flow respectively. The continuity equation (1.b) is also known as the incompressibility condition. If the flow does not depend on the temperature the coupling with $(1.c)$ disappears and $\mathbf{f}$ does not depend on θ, then $(1.a-1.b)$ give the Navier-Stokes equations for isothermal flows. The dimensionless parameters Re, Ra and Pr represent the Reynolds, Rayleigh and Prandtl numbers.

The system must be supplemented with initial conditions, for instance $\theta(\mathbf{x}, 0) = \theta_o(\mathbf{x})$ and $\mathbf{u}(\mathbf{x}, 0) = \mathbf{u}_o(\mathbf{x})$ in Ω and with boundary conditions, say $\mathbf{u} = \mathbf{g}$ and $B\theta = 0$ on Γ, $t \geq 0$, where B is a temperature boundary operator which can involve Dirichlet, Neumann or mixed boundary conditions.

The difficulties of the system are: the non linearity of the equations, the coupling among them, there is not enough information to compute the pressure and to satisfy the incompressibility condition. A convenient semi-implicit time discretization combined with an operator splitting, solving simpler subproblems, may be used to overcome these obstacles.

NUMERICAL PROCEDURE

The time derivatives in (1.a) and (1.c) are approximated by the second-order finite differences

$$h_t(\mathbf{x}, (n+1)\Delta t) = \tfrac{3h^{n+1} - 4h^n + h^{n-1}}{2\Delta t} \qquad (2)$$

with $n \geq 1$, $\mathbf{x}\,\epsilon\,\Omega$; where $h^r \equiv h(\mathbf{x}, r\Delta t)$ and Δt, the time step.

Thus, the corresponding semi-discrete problem for system (1), in Ω, reads

$$\begin{aligned} &\tfrac{\frac{3}{2}\mathbf{u}^{n+1} - 2\mathbf{u}^n + \frac{1}{2}\mathbf{u}^{n-1}}{\Delta t} + 2(\mathbf{u}\cdot\nabla\mathbf{u})^n \\ &\quad -(\mathbf{u}\cdot\nabla\mathbf{u})^{n-1} + \nabla p^{n+1} = \tfrac{1}{Re}\nabla^2\mathbf{u}^{n+1} \\ &\qquad\qquad + \mathbf{f}^{n+1}, \qquad (a)\\ &\nabla\cdot\mathbf{u}^{n+1} = 0, \qquad (b) \qquad (3)\\ &\tfrac{3\theta^{n+1} - 4\theta^n + \theta^{n-1}}{2\Delta t} + 2(\mathbf{u}\cdot\nabla\theta)^n \\ &\quad -(\mathbf{u}\cdot\nabla\theta)^{n-1} = \tfrac{1}{RePr}\nabla^2\theta^{n+1}. \qquad (c) \end{aligned}$$

as it can observed, the non-linear terms $(\mathbf{u}\cdot\nabla)\mathbf{u}$ and $(\mathbf{u}\cdot\nabla)\theta$, in (1.a) and (1.c), are approximated with a linear extrapolation of the values of the two previous time levels.

Then, following closely [1] and [2], the operator splitting of four step that is applied at each time level is given by

Step 1)

$$\begin{aligned} &\tfrac{3\theta^{n+1} - 4\theta^n + \theta^{n-1}}{2\Delta t} - \tfrac{1}{RePr}\nabla^2\theta^{n+1} \\ &= -2(\mathbf{u}^n\cdot\nabla)\theta^n + (\mathbf{u}^{n-1}\cdot\nabla)\theta^{n-1} \;\; in \;\; \Omega \\ &\qquad B\theta^{n+1}|_\Gamma \;=\; 0 \end{aligned}$$

Step 2)

$$\begin{aligned} &\tfrac{\mathbf{u}^* - 2\mathbf{u}^n + \frac{1}{2}\mathbf{u}^{n-1}}{\Delta t} = -2(\mathbf{u}^n\cdot\nabla)\mathbf{u}^n + \\ &(\mathbf{u}^{n-1}\cdot\nabla)\mathbf{u}^{n-1} + \tfrac{Ra}{PrRe^2}\theta^{n+1}\mathbf{e} \;\; in \;\; \Omega, \qquad (4) \end{aligned}$$

Step 3)

$$\tfrac{\mathbf{u}^{**} - \mathbf{u}^*}{\Delta t} \;=\; -\nabla p^{n+1} \qquad in \;\; \Omega,$$

Step 4)

$$\begin{aligned} &\tfrac{\frac{3}{2}\mathbf{u}^{n+1} - \mathbf{u}^{**}}{\Delta t} \;=\; \tfrac{1}{Re}\,\nabla^2\mathbf{u}^{n+1} \qquad in \;\; \Omega \\ &\qquad \mathbf{u}^{n+1}|_\Gamma = \mathbf{g}, \end{aligned}$$

where $\mathbf{f}^{n+1}$ has been replaced by $\frac{Ra}{PrRe^2}\theta^{n+1}\mathbf{e}$; $\mathbf{u}^*$ and $\mathbf{u}^{**}$ are intermediate velocities, the latter satisfies the incompressibility condition

$$\nabla\cdot\mathbf{u}^{**} = 0 \qquad (5)$$

Taking the divergence in step 3), using (5), an equation of Poisson type for the pressure is obtained, in Ω,

$$\nabla^2 p^{n+1} = \tfrac{1}{\Delta t}\mathbf{u}^*, \qquad (6)$$

for which a convenient Neumann boundary condition can be determined by taking the normal component in the semi-discrete momentum equation (3.a)

$$\begin{aligned} &\tfrac{\partial p^{n+1}}{\partial\mathbf{n}} = \mathbf{n}\cdot[\tfrac{1}{\Delta t}(-\tfrac{3}{2}\mathbf{u}^{n+1} + 2\mathbf{u}^n - \tfrac{1}{2}\mathbf{u}^{n-1}) \\ &-2((\mathbf{u}^n\cdot\nabla)\mathbf{u}^n + \tfrac{1}{Re}\nabla\times(\nabla\times\mathbf{u}^n)) + \qquad (7)\\ &((\mathbf{u}^{n-1}\cdot\nabla)\mathbf{u}^{n-1} + \tfrac{1}{Re}\nabla\times(\nabla\times\mathbf{u}^{n-1}) \\ &+\tfrac{Ra_l}{PrRe^2}\theta^{n+1}\mathbf{e}] \;\; on \;\; \Gamma. \end{aligned}$$

In (7) can be observed that the laplacian of the velocity has been substituted by the double curl of $\mathbf{u}$, using the identity $\nabla^2\mathbf{u} = \nabla(\nabla\cdot\mathbf{u}) - \nabla\times\nabla\times\mathbf{u}$ with the incompressibility condition, and then applying a linear extrapolation of the two previous time levels.

It is known that elliptic problems with Neumann boundary condition, like the one given by (6) and (7), do not have a unique solution, it is unique only within an arbitrary constant if a compatibility condition holds, [2], Glowinski [6], and Temam [7]. It is also known, see for instance [7] that the pressure equation with Neumann boundary condition $\frac{\partial p^{n+1}}{\partial\mathbf{n}}|_\Gamma = 0$ is equivalent that $\mathbf{u}^{**}$ be the projection of $\mathbf{u}^*$ onto the divergence-free subspace of vector fields, provided that $\mathbf{u}^{**}|_\Gamma = \mathbf{0}$ which, in our case, does not have any influence in the calculation of $\mathbf{u}^{**}$ in step 2; however, as pointed out by some authors $\frac{\partial p^{n+1}}{\partial\mathbf{n}}|_\Gamma = 0$ is not good neither for numerical purposes [2] nor to satisfy the exact pressure [7].

It should noted: In step 1) (temperature step) the temperature θ^{n+1} is computed; in steps 2)-4) (motion steps), $\mathbf{u}^*$

is computed in step 2), then the pressure p^{n+1} is computed in step 3) through the Poisson equation (6) with Neumann boundary condition (7), once p^{n+1} has been computed the intermediate velocity $\mathbf{u}^{**}$, to be used in step 4), is computed in step 2); finally the velocity $\mathbf{u}^{n+1}$ is computed in step 4).

Thus, we must solve two elliptic scalar problems to obtain θ^{n+1}, p^{n+1} and a vectorial one, with Dirichlet boundary condition, to obtain $\mathbf{u^{n+1}}$, whereas the intermediate velocities, $\mathbf{u}^*$ and $\mathbf{u}^{**}$, are computed explicitly. For isothermal flows the temperature step is not considered. It must be noted that the scheme is independent of the spatial dimension and of the shape of the region Ω.

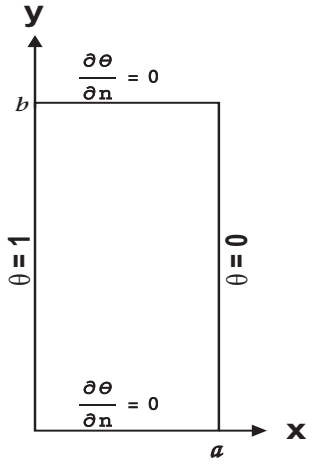

FIG. 1: Geometry of the model

In this work, 2D numerical experiments taking place on rectangular cavities $\Omega = (0, a) \times (0, b)$ are reported. Then, the second order approximation (2) on boundary points and central finite differences in interior points are used to discretize the right hand side terms. The elliptic problems are solved with the second order approximation option, based on finite differences, of the Fishpack solver [8], which uses an efficient cyclic reduction iterative method to solve the corresponding algebraic linear systems, [9], and the non-uniqueness of the pressure partial differential problem is handled through a weighted minimal least square solution on the algebraic system.

Once the final velocity $\mathbf{u}$ is obtained, at each time level, the vorticity ω and the stream function ψ are computed through the relations

$$\omega = ||\nabla \times \mathbf{u}|| \qquad in \;\; \Omega$$
$$\nabla^2 \psi = -\omega \qquad in \;\; \Omega$$

The heat tranfer on the hot wall, of natural convection flows, is measured with the local, $Nu(y)$, and global, $\overline{Nu}$, Nusselt numbers, defined by

$$Nu(y) = \tfrac{\partial \theta}{\partial x}|_{x=0} \qquad \text{and}$$
$$\overline{Nu} = \tfrac{1}{b} \int_0^b Nu(x) dx \;;$$

the derivative is approximated by (2) and the integral by the second order trapezoidal rule.

NUMERICAL RESULTS

For natural convection the walls of the cavity are fixed and solid, then by viscosity the boundary condition for the velocity is $\mathbf{u} = \mathbf{0}$; the one for the temperature, given so far implicitly on the boundary operator B, is given by

$$\theta|_{x=0} = 1, \quad \theta|_{x=a} = 0; \quad \tfrac{\partial \theta}{\partial n}|_{y=0,b} = 0$$

which means that the left wall is the hot wall, the right wall is the cold one, and the horizontal walls are insulated, Figure 1 shows the geometry of the model; the respective initial conditions for the velocity and the temperature are $\mathbf{u}_o(\mathbf{x}) = (0, 0)$ and $\theta(\mathbf{x}) = 0$. For isothermal flows, the lid-driven cavity problem is considered, then the $\mathbf{u}$ boundary condition is $\mathbf{u} = (1, 0)$ on the moving wall, $y = b$, and $\mathbf{u} = \mathbf{0}$ elsewhere; the initial condition is the same of natural convection flows. In both cases flows at the steady state, based on the absolute stopping criterion in all the cavity, Báez and Nicolás [10] and Nicolás and Bermúdez [11], with tolerance 10^{-5}, are reported in terms of the isotherms and/or the streamlines and the isocontours of the vorticity.

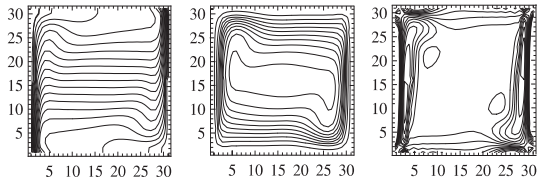

FIG. 2: $Ra = 10^6$, $A = 1$, $\Delta t = 10^{-5}$, $h = 1/30$ and $T_{ss} = .1167$

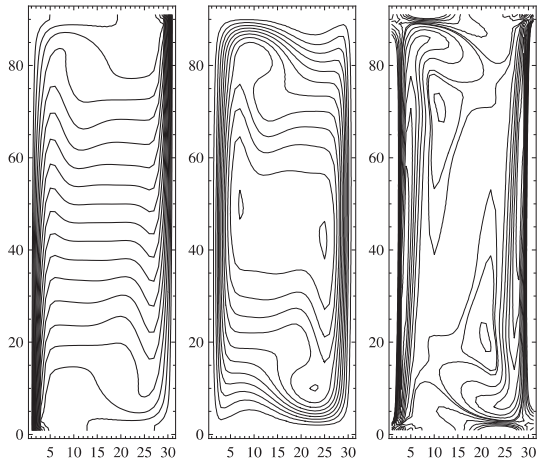

FIG. 3: $Ra = 10^6$, $A = 3$, $\Delta t = 10^{-5}$, $h_x \times h_y = 1/30 \times 3/90$ and $T_{ss} = .2243$

For natural convection flows $Re = 1$, Gunsburguer [12], and the results are obtained in cavities filled with air, $Pr = 0.71$, and $Ra = 10^6$ and 10^7; some comments for $Ra = 10^4$ and $Ra = 10^5$ are made. For isothermal flows, the case with $Re = 1000$ is studied. Rectangular cavities with aspect ratio A=1 and 3 are considered for both cases. The discretization parameters, mesh sizes $h_x \times h_y$ ($h = h_x = h_y$) and the time step Δt, will be indicated in each case under study.

Results for natural convection with $Ra = 10^6$ and $A = 1$ are presented in Figure 2. The isotherms tend to adhere

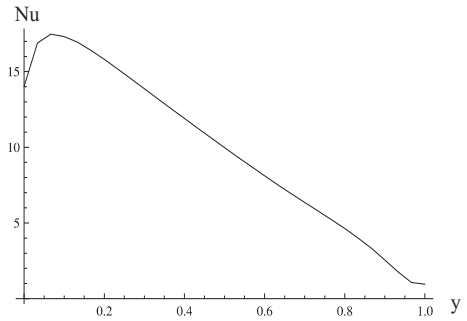

FIG. 4: local Nusselt number for $Ra = 10^6$ and $A = 1$

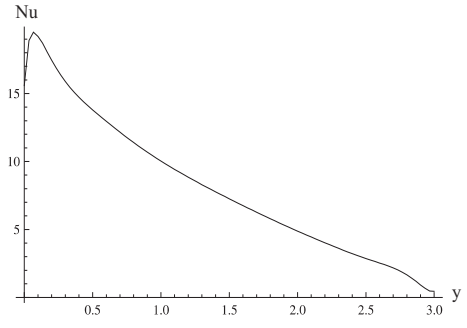

FIG. 5: local Nusselt number for $Ra = 10^6$ and $A = 3$

towards the vertical walls which leads a high heat transfer on the hot wall. This situation influences on the streamlines and on the isocontours of the vorticity, since the first ones are more concentrated near the lateral walls, which indicates a strong motion of the fluid, whereas the second ones show areas of high activity near the boundary walls; these results show concordance with those obtained in [10] and by Henkes and Hoogendoorn [13]. If the aspect ratio increases to $A = 3$, Figure 3, a very similar behaviour to the former is observed, however some distortions appear in the isotherms, streamlines and isocontours of the vorticity close to the left upper and the right lower corners due to the interaction against the top and bottom walls of the hot fluid going up and the cold one going down. It can be observed, from Figures 4 and 5, that the respective maximum of the local heat transfer, is located near the lower corner of the hot wall, but this value is slightly higher for $A = 3$ than that one for $A = 1$.

Table I. Comparison of some results for $Ra = 10^6$.

Ref.	$\|\psi\|_{max}$	$\overline{Nu}$	Nu_{max}	Nu_{min}
[14]	20.914	9.027	14.215	1.749
[15]	-	8.754	17.872	1.232
(T)	19.934	9.892	17.381	0.983

For $Ra = 10^6$ with $A = 1$, in Table I, a comparison is made of some numerical values between our results (T) and those obtained by Vahl Davis [14], using $h = \frac{1}{20}$, and by Markatos and Pericleous [15]; these two works use another formulation of the problem and a different numerical approach. In Table II, the corresponding results for $Ra = 10^7$ with $A = 1$ are compared with those obtained by Lequéré [16]; neither [14] nor [15] reports numerical values for this Ra.

Some of the results show good agreement since the differences are less than 10 %; however, some of them show a

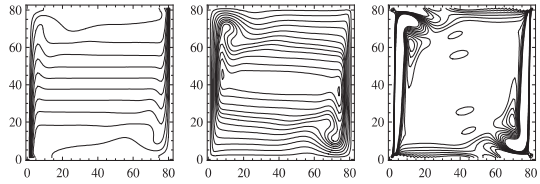

FIG. 6: $Ra = 10^7$, $A = 1$, $\Delta t = 10^{-6}$, $h = 1/80$ and $T_{ss} = .07674$

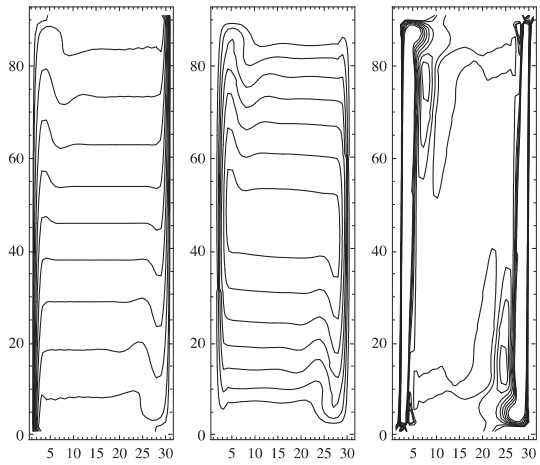

FIG. 7: $Ra = 10^7$, $A = 3$, $\Delta t = 10^{-6}$, $h_x \times h_y = 1/30 \times 3/90$ and $T_{ss} = 0.1443$

significant difference, mainly the global Nusselt number $\overline{Nu}$ compared with [16] in Table II.

Table II. Comparison of some results for $Ra = 10^7$.

Ref.	$\|\psi\|_{max}$	$\overline{Nu}$	Nu_{max}	Nu_{min}
[16]	-	16.523	39.395	1.366
(T)	47.162	18.620	39.153	1.303

For $Ra = 10^7$, from Figures 6 - 9 a more vigorous motion of the fluid is obtained since the isotherms, the streamlines, and the isocontours of the vorticity show a more remarkable adherence to the vertical walls of the cavity than those observed for $Ra = 10^6$; on the other hand, the respective local Nusselt number, for $A = 1$ and $A = 3$, indicate that the local heat transfer has been increased also.

Table III. Results for $Ra = 10^6$ and 10^7 with $A = 3$.

Ra	$\|\psi\|_{max}$	$\overline{Nu}$	T_{ss}
10^6	47.162	8.115	0.224
10^7	71.379	15.254	0.134

Table III shows the values of $|\psi|_{max}$, $\overline{Nu}$ and T_{ss} of our results for $Ra = 10^6$ and 10^7 with $A = 3$.

About our results in Tables I, II and III it is observed that when Ra increases, with A fixed, the motion of the fluid and the global heat transfer, measured by ψ and $\overline{Nu}$ respectively, are also increased, but the time to reach the steady state T_{ss} diminishes. On the other hand, although the motion of the fluid is also stronger when A increases, with Ra fixed, the global Nusselt number decreases. This last behaviour, when

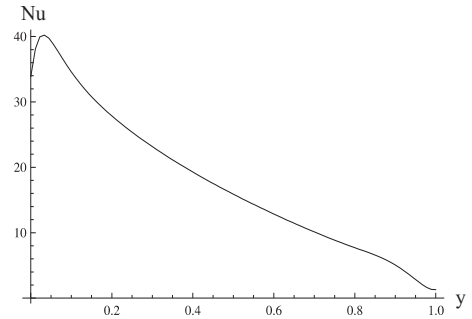

FIG. 8: local Nusselt number for $Ra = 10^7$ and $A = 1$

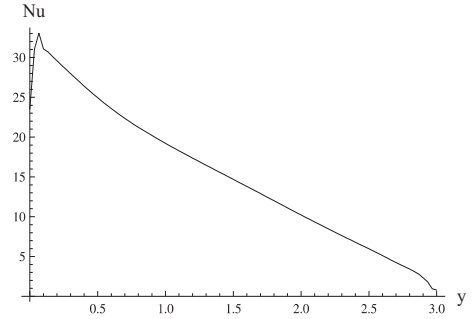

FIG. 9: local Nusselt number for $Ra = 10^7$ and $A = 3$

$A = 2$, occurs also for $Ra = 10^5$, ; however, for $Ra = 10^4$, it is observed that $|\psi|_{max}$ and $\overline{Nu}$ have increased when $A = 2$, but when $A = 3$, although $|\psi|_{max}$ increases, $\overline{Nu}$ diminishes. This flow pattern, until $A = 2$, occurs also with the velocity-vorticity formulation; Table IV shows the comparison with the results of such formulation in Bermúdez and Nicolás [17]. It must be noted that our results (T)in Table IV are obtained with mesh sizes $h_x = \frac{1}{24} \times h_y = \frac{1}{24}$, $h_x = \frac{1}{24} \times h_y = \frac{2}{48}$, and $h_x = \frac{1}{24} \times h_y = \frac{3}{72}$, all of them with $\Delta t = 0.0001$, whereas those in [17] with $h_x = \frac{1}{64} \times h_y = \frac{1}{64}$, $\Delta t = 0.0001$, and $h_x = \frac{1}{64} \times h_y = \frac{2}{128}$, $\Delta t = 0.00001$, respectively.

Table IV. Results for $Ra = 10^4$ with $A = 1$.

Ref.	A	$\lvert\psi\rvert^{mid}$	$\overline{Nu}$
[17]	1	7.515	2.259
(T)	1	6.976	2.265
[17]	2	10.160	2.363
(T)	2	13.201	2.383
[17]	3	-	-
(T)	3	17.520	2.262

For isothermal flows, Figures 10 and 11 show results with $Re = 1000$ and $A = 1,\ 3$ respectively; for those in the square cavity, one primary and two secondary vortices appear in the streamlines while three primary vortices and one small secondary vortex only, in the right lower corner, for $A = 3$; the isocontours of the vorticity indicate a high activity in almost all the zone around the center when $A = 1$, and in the upper region, near of the moving wall for $A = 3$. Results for the square cavity show very good concordance with those obtained by Ghia et al. [18] and with the streamlines reported by Erturk (the isocontours of the vorticity are no showed in this work) [19]; for $A = 3$ the results in this work show a very good agreement with those obtained by Nicolás and Bermúdez [11], except in this last work, the small secondary vortex appears in the left lower corner. In all those works we are comparing with finer meshes than ours are used.

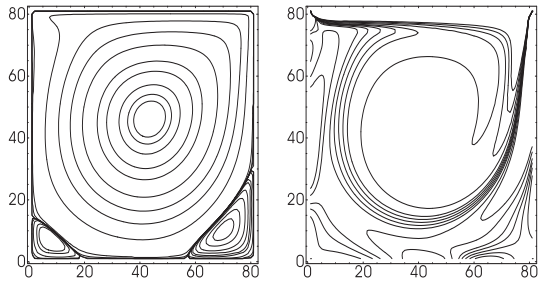

FIG. 10: $Re = 1000$, $h = \frac{1}{80}$, $\Delta t = 0.01$, $T_{ss} = 31.15$

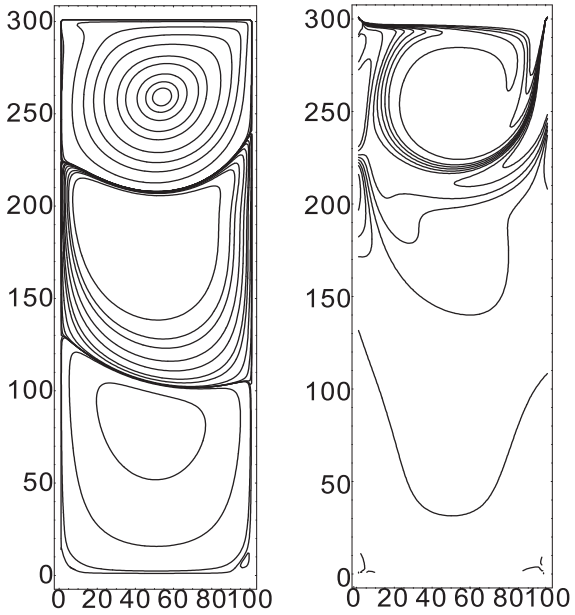

FIG. 11: $Re = 1000$, $A = 3$, $h_x \times h_y = \frac{1}{100} \times \frac{3}{300}$, $\Delta t = 0.0001$ and $T = 150$

CONCLUSIONS

The numerical results obtained by applying a simple projection method to the mathematical model of natural convection/isothermal flows, formulated in terms of the primitive variables, indicate that the scheme is able to reach steady state flows, as those shown here, for moderate values of Ra or Re, and aspect ratios $A \leq 3$; preliminary results show that it is also possible to obtain satisfactory results, for steady state or time depending flows of higher values of Ra or Re, and of A with coarser meshes than those used by other authors using other methods, either in stream function-vorticity variables, [11], or in velocity-vorticity variables, [17]; on this matter, is remarkable the difference in mesh size of our natural convection flows as well as the isothermal ones, in particular with those in [17], as Table IV shows, for $Ra = 10^4$, obtaining nevertheless the same conclusion until $A = 2$ about $\overline{Nu}$, and

given some indication, because of $A = 3$, that if A would increase then $\overline{Nu}$ may be oscillatory. For thermal fluids, the effect of increasing one of the two values, Ra or A, and the other fixed, is observed on the fluid motion, on the heat transfer, and on the time to reach the steady state. For isothermal flows, the corresponding effect on the fluid motion and on the time to reach the steady state is shown only for the case when A increases and $Re = 1000$ fixed. Although in this work only 2D fluid flows are reported, the numerical procedure can be applied to 3D problems and there is not problem at all to extend the scheme to mixed convection thermal problems.

REFERENCES

[1] Badalassi V. E., Ceniceros H. D., Banerjee S., Computation of multiphase systems with phase field models, it J. of Comp. Physics, Vol. 190. 2003, pp. 371-397.

[2] Karnadiakis G. E., Israeli M. and Orszag S. A., High-order splitting methods for the incompressible Navier-Stokes equations, *J. of Comp. Physics*, Vol. 97, 1991, pp. 414-427.

[3] Orszag S., Israeli M., Deville M., Boundary conditions for incompressible flows, *J. of Scientific Computing*, Vol. 1, 1986, pp. 75-111.

[4] Gresho P. and Sani R., On pressure boundary conditions for incompressible Navier-Stokes equations, *Int. J. for Num. Meth. in Fluids*, Vol. 7, 1987, pp. 1111-1145.

[5] Sani R. L., Shen J., Pironneau O., Gresho P. M. Pressure boundary condition for the time-dependent incompressible Navier-Stokes equations. *International Journal for Numerical Methods in Fluids* 2006; **50**:673-682.

[6] Glowinski R. *Numerical Methods for Non-Linear Variational Problems*. Springer: Berlin, 1984.

[7] Temam R. *Navier-Stokes Equations, Theory and Numerical Analysis*. AMS CHELSEA PUBLISHING: Providence RH., USA, 2001.

[8] Adams J., Swarztrauber P. and Sweet R., FISHPACK: A Package of Fortran Subprograms for the Solution of Separable Elliptic PDE's, *The National Center for Atmospheric Research, Boulder*, Colorado, 1980.

[9] Sweet R., A cyclic reduction algorithm for solving block tridiagonal systems of arbitrary dimensions, *SIAM Journal on Numer. Anal.*, Vol. 14, 1977, pp. 706-720.

[10] Báez E. and Nicolás A., 2D natural convection flows in tilted cavities: porous media and homo geneous fluids, *Int. J. of Heat and Mass Transfer*, Vol. 49, 2006, pp. 4773-4785.

[11] Nicolás A. and Bermúdez B., 2D thermal/isothermal incompressible viscous flows, *Int. J. Numer. Meth. Fluids*, Vol. 48, 2005, pp. 349-366.

[12] Gunzburger M. D., Finite Element Methods for Viscous Incompressible Flows: A guide to theory, practice, and algorithms, *Academic Press, INC.*, 1989.

[13] Henkes R. A. W. M. and Hoogendoorn C. J., Scaling of laminar natural-convection flow in a heated square cavity. *Int. J. Heat and Mass Transfer*, Vol. 36 (11), 1993, pp. 2913-2925.

[14] De Vahl Davis G., Natural convection of air in a square cavity: a bench mark numerical solution. *International Journal for Numerical Methods in Fluids*, Vol. 3, 1983, pp. 249-264.

[15] Markatos N. C. and Pericleous K.A., Laminar and turbulent natural convection in an enclosed cavity, *Int. J. Heat and Mass Transfer* Vol. 27 (5), 1984, pp. 755-772.

[16] Le Quéré P., Accurate solutions to the square thermally dirven cavity at high Rayleigh number. *Computers & Fluids*, Vol. 20 (1),1991, pp. 29-41.

[17] Bermúdez B. and Nicolás A., Natural convection/isothermal viscous incompressible flows by the velocity-vorticity formulation. *Paper BB1, Hefat2008* Proceedings.

[18] Ghia U., Ghia N., Shin C. T., High-Re solutions for incompressible flow using the Navier-Stokes equations and a multigrid method. *Journal of Computational Physics*, Vol. 48, 1982, pp. 387-411.

[19] Erturk E., Corke, T. C. and Gökçöl C., Numerical solutions of 2-D steady incompressible driven cavity flow at high Reynolds numbers. *International Journal for Numerical Methods in Fluids*, Vol. 48, 2005, pp. 747-774.